

Color shift in $\text{Al}_2\text{O}_3 \cdot x\text{Cr}_2\text{O}_3$ solid solutions and the electroneutrality principle

J. M. García-Lastra,¹ M. T. Barriuso,² J. A. Aramburu,³ and M. Moreno³

¹*Departamento de Física de Materiales, Facultad de Químicas, Universidad del País Vasco, 20018 San Sebastián, Spain*

²*Departamento de Física Moderna, Universidad de Cantabria, 39005 Santander, Spain*

³*Departamento de Ciencias de la Tierra y Física de la Materia Condensada, Universidad de Cantabria, 39005 Santander, Spain*

(Received 21 April 2009; revised manuscript received 2 June 2009; published 16 June 2009)

Although the series of $\text{Al}_2\text{O}_3 \cdot x\text{Cr}_2\text{O}_3$ compounds is a model system among mixed crystals the actual origin of the progressive color change from red to green upon increasing the chromium content is not clarified yet. It is shown in this work that such a color shift for $x < 0.2$ mainly comes from the reduction in the internal electric field, experienced by the CrO_6^{9-} complex, due to the progressive replacement of a close Al^{3+} ion by Cr^{3+} as a result of the electroneutrality principle. The proposed model accounts for the color shift along the whole series.

DOI: 10.1103/PhysRevB.79.241106

PACS number(s): 71.55.-i, 61.72.Bb, 71.15.Mb, 91.60.Mk

In the search of materials displaying a particular property great attention is focused on the series of mixed crystals where the physico-chemical properties are modified by simply changing the composition even if the crystal structure is kept.¹⁻³ As an example, in the case of insulating solid solutions containing transition-metal cations such as $\text{Al}_2\text{O}_3 \cdot x\text{Cr}_2\text{O}_3$ ($0 < x < 1$), $\text{CoAl}_2\text{O}_4 \cdot x\text{CoCr}_2\text{O}_4$, or $\text{PbCrO}_4 \cdot x\text{PbMoO}_4 \cdot y\text{PbSO}_4$ the color dependence on the composition is used for preparing different inorganic pigments.^{2,4-6} Although the change in a given property along a series of insulating mixed crystals is of interest for applications, the main origin of this fact is often not well established. This situation has already been encountered looking at the series of $\text{Al}_2\text{O}_3 \cdot x\text{Cr}_2\text{O}_3$ mixed crystals which has widely been investigated⁵⁻⁷ and thus can be considered as a model system within the realm of insulating solid solutions. Although 50 years ago it was already established that in that series there is a progressive color change from red to green upon increasing the chromium content,⁵ the actual origin of this shift is not understood yet. A similar color shift has also been observed along the series of $\text{MgAl}_2\text{O}_4 \cdot x\text{MgCr}_2\text{O}_4$ and $\text{YAl}_2\text{O}_4 \cdot x\text{YCr}_2\text{O}_4$ mixed crystals^{5,6} where crystal structure is also kept.

The present work deals with this unsolved problem. As a central issue we propose that the color change in the $\text{Al}_2\text{O}_3 \cdot x\text{Cr}_2\text{O}_3$ series is mainly related to the electroneutrality principle by Pauling for a transition-metal complex,⁸ stating that the total charge of the transition-metal cation in the complex is *nearly* zero.

The color of Cr^{3+} -based gemstones, as ruby ($\text{Al}_2\text{O}_3 \cdot \text{Cr}^{3+}$), emerald ($\text{Be}_3\text{Si}_6\text{Al}_2\text{O}_{18} \cdot \text{Cr}^{3+}$), or chromium spinel ($\text{MgAl}_2\text{O}_4 \cdot \text{Cr}^{3+}$), is essentially governed by the energy of the first spin allowed ${}^4A_g(t_{2g}^3) \rightarrow {}^4T_{2g}(t_{2g}^2e_g)$ transition of the CrO_6^{9-} complex, which is just equal to the cubic field splitting parameter, $10Dq$.⁹ Therefore, within the widely used ligand field theory, the color shift in $\text{Al}_2\text{O}_3 \cdot x\text{Cr}_2\text{O}_3$ mixed crystals can be ascribed to an increase in the mean $\text{Cr}^{3+}\text{-O}^{2-}$ distance, R , in the complex that it is well known to produce a reduction in the $10Dq$ value.¹⁰⁻¹² However, recent extended x-ray absorption fine structure (EXAFS) data on the series of $\text{Al}_2\text{O}_3 \cdot x\text{Cr}_2\text{O}_3$ crystals¹³ cast serious doubts on this traditional interpretation. Indeed such measurements reveal that R experiences an increase of only 0.75% on passing

from ruby ($R = 196.5$ pm) to Cr_2O_3 while, within the experimental uncertainty of ± 0.5 pm, it is apparently constant in the $0 < x < 0.25$ range. However, looking at the experimental $10Dq$ values,^{6,9,14} they already move from $18\,070\text{ cm}^{-1}$ for ruby ($x \leq 0.005$) to $17\,450\text{ cm}^{-1}$ for $x = 0.25$, while $10Dq = 16\,650\text{ cm}^{-1}$ for $x = 1$. The present work is aimed at clarifying the actual origin of this surprising phenomenon.

An insight into the electronic properties due to a transition-metal impurity in an insulating crystal is greatly helped by the *localization* of active electrons in the complex formed with anion ligands. In the case of $\text{MgAl}_2\text{O}_4 \cdot \text{Cr}^{3+}$ (Ref. 15) and $\text{Al}_2\text{O}_3 \cdot \text{Cr}^{3+}$ (Ref. 16) the localization is supported by electron nuclear double resonance (ENDOR) data on nearest Al nuclei to the CrO_6^{9-} complex which show that the electronic density of three unpaired electrons on such nuclei is actually negligible. By virtue of this fact it has often been assumed that the actual $10Dq$ value can be explained considering only the CrO_6^{9-} complex *in vacuo*. Although the dominant contribution to $10Dq$ already appears considering the isolated complex [termed $(10Dq)_V$] there is, however, another supplementary contribution (termed Δ_R), which is often ignored, thus implying that $10Dq = (10Dq)_V + \Delta_R$.^{11,17,18} Indeed as the complexes are never isolated but embedded in an insulating lattice, they also necessarily feel the electric field, $E_R(\mathbf{r})$, arising from the *rest* of the ions involved in the host lattice which modifies the energy of electronic states of the complex and thus $10Dq$. This supplementary contribution to $10Dq$, Δ_R , has been shown to be the main responsible for the distinct color exhibited by Cr^{3+} in oxides with *different* crystal structure,^{17,18} and also the different $10Dq$ value found experimentally for Mn^{2+} in cubic KMgF_3 and LiBaF_3 lattices despite the $\text{Mn}^{2+}\text{-F}^-$ distance is found to be practically the same in both systems.¹⁹ In the case of ruby it has been found that $(10Dq)_V = 16\,000\text{ cm}^{-1}$ and $\Delta_R = 2100\text{ cm}^{-1}$.^{11,17,18} As $\Delta_R > 0$ for ruby these ideas, together with the EXAFS data¹³ on the series of $\text{Al}_2\text{O}_3 \cdot x\text{Cr}_2\text{O}_3$ mixed crystals, strongly suggest that the decrease in $10Dq$ already observed in the $0 < x < 0.25$ range might be ascribed mainly to a progressive decrement of Δ_R when the chromium content increases.¹⁸

In highly dilute samples of $\text{Al}_2\text{O}_3 \cdot \text{Cr}^{3+}$ all cations close to a given CrO_6^{9-} complex are Al^{3+} ions whose actual charge has been shown to be not far from $+3e$.²⁰ However, when the chromium content in the series of $\text{Al}_2\text{O}_3 \cdot x\text{Cr}_2\text{O}_3$ crystals in-

creases some of the close sites can be occupied by a Cr^{3+} ion substituting Al^{3+} . The central idea of our model is that the actual charge of chromium cations in CrO_6^{9-} complexes is much smaller than that corresponding to aluminum in AlO_6^{9-} complexes because Cr^{3+} is an open shell ion, and thus it can receive *additional* electronic charge from closed shell oxygen ligands (dative bonding). This idea is essentially behind Pauling's electroneutrality principle applied to transition-metal complexes, stating that the total charge of the transition-metal cation is *nearly* zero.⁸ It is worth noting that on passing from AlO_6^{9-} to an isolated CrO_6^{9-} complex there are six O^{2-} ions giving electronic charge to chromium, a fact which implies a smaller variation in the ligand charge. Therefore, the replacement of Al^{3+} ions by Cr^{3+} ones along the $\text{Al}_2\text{O}_3 \cdot x\text{Cr}_2\text{O}_3$ series would give rise to a decrease in the associated electric field on each CrO_6^{9-} complex, $\mathbf{E}_R(\mathbf{r})$, which in turn is expected to reduce the Δ_R contribution to $10Dq$, thus favoring the transparency to the green light.

Seeking to explore the reliability of this idea we have first calculated the actual charge of the cation, q_c , for pure Al_2O_3 and Cr_2O_3 lattices which exhibit the same crystal structure. To this end, density functional theory (DFT)-based calculations have been performed on $M_{27}\text{O}_{42}^{3-}$ superclusters ($M=\text{Al}$ and Cr) formed by a M ion and its first 68 neighbors in a $M_2\text{O}_3$ lattice.²¹ Values of q_c have been derived using the Bader charge analysis as it is implemented in the Amsterdam density functional (ADF) code.²² The obtained values are $q_c=2.6e$ for Al_2O_3 and $q_c=1.3e$ for Cr_2O_3 , pointing out that there is a strong reduction in the total charge of the cation when aluminum is replaced by chromium.

In a second step we have calculated what is the $10Dq$ value corresponding to the CrO_6^{9-} complex embedded in Al_2O_3 when one or more Al^{3+} ions are replaced by Cr^{3+} ions. The procedure for calculating $10Dq$ is the same one previously employed in the study of several gemstones.^{11,17,18} Accordingly, $10Dq$ is derived by means of DFT calculations, considering the CrO_6^{9-} complex at the right equilibrium geometry and subject to the internal field, $\mathbf{E}_R(\mathbf{r})$, coming from the host lattice. The electrostatic potential, $V_R(\mathbf{r})$, generating $\mathbf{E}_R(\mathbf{r})$ has been derived using a mixed Ewald-Evjen method described elsewhere.^{11,17,18}

Let us consider an aluminum ion in Al_2O_3 . The nearest Al^{3+} ion is at 265 pm and placed along the C_3 axis. Only a little further there are three Al^{3+} ions at 279 pm but lying in the perpendicular plane to the principal axis (Fig. 1). The rest of the Al^{3+} ions are located at a distance higher than 320 pm.

As shown in Table I, the calculated $10Dq$ value for ruby is 17 917 cm^{-1} using $q_c=2.6e$ for Al^{3+} ions. However, a significant decrease of 406 cm^{-1} is already obtained when only one of the three close Al^{3+} ions lying in the perpendicular plane to the C_3 axis is replaced by Cr^{3+} ($q_c=1.3e$) keeping the same R value. This variation thus means a 20% reduction in Δ_R . The lessening in $10Dq$ is found to amount only to 40 cm^{-1} when Cr^{3+} substitutes the Al^{3+} ion placed along the C_3 axis. When any Al^{3+} ion lying at a distance higher than 320 pm is replaced by Cr^{3+} , we have verified that the change in $10Dq$ is always smaller than 40 cm^{-1} and usually does not exceed 20 cm^{-1} .

Bearing in mind these facts we have tried to understand the experimental dependence of $10Dq$ on x under the follow-

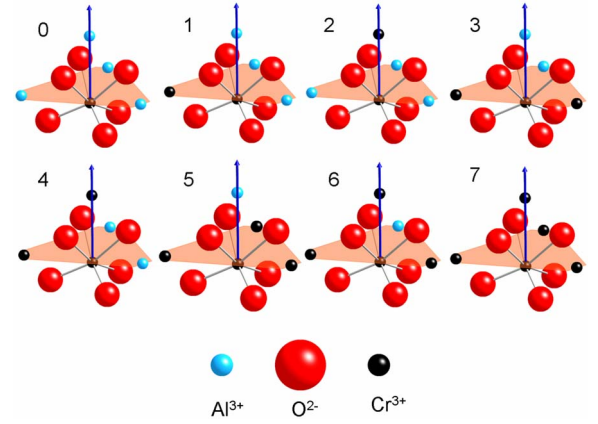


FIG. 1. (Color online) Case 0: CrO_6^{9-} complex in Al_2O_3 and its first four Al^{3+} neighbor ions. One of the Al^{3+} ions is placed at the C_3 axis of the complex (blue arrow), whereas the other three ones are placed at equivalent positions in the perpendicular plane to that axis which contains the Cr ion of the complex (red plane). Cases 1, 2, 3, 4, 5, 6, and 7 correspond to the different possible arrangements when one (cases 1 and 2), two (cases 3 and 4), three (cases 5 and 6), or four (case 7) Al^{3+} neighbor ions are replaced by Cr^{3+} ions in $\text{Al}_2\text{O}_3 \cdot x\text{Cr}_2\text{O}_3$ mixed crystals.

ing assumptions: (i) only the complexes having at least one of the four nearest Al^{3+} ions replaced by Cr^{3+} have a $10Dq$ value different from that corresponding to ruby. (ii) The incorporation of Cr^{3+} ions into the lattice sites obeys a statistical criterion, an assumption strongly supported by EXAFS data on the $\text{Al}_2\text{O}_3 \cdot x\text{Cr}_2\text{O}_3$ series.¹³ Such experimental results show that for any x value the EXAFS spectra cannot be understood as a weighted superposition of those corresponding to ruby and Cr_2O_3 but through a progressive incorporation of Cr^{3+} into the lattice when its content increases.

According to these reasonable but simplifying assumptions, for calculating the actual $10Dq$ value for a given Cr^{3+} concentration it is only necessary to perform the statistical average of the eight *centers* shown in Fig. 1. In other words,

$$10Dq = \sum_{j=0}^7 p_j [10Dq(R_j)]. \quad (1)$$

Here p_j means the probability for the occurrence of the j center (where $j=0$ actually corresponds to ruby) for a given x value, while R_j denotes the associated mean Cr^{3+} - O^{2-} distance. The equilibrium distance for the j center has been derived through an interpolation between the values $R=196.5$ pm and $R=198.0$ pm measured for ruby and Cr_2O_3 , respectively.²³ The difference between $[10Dq(R_j)]_j$ and the corresponding $10Dq$ calculated for $R_0=196.5$ pm has been taken from the R dependence of $10Dq$ for ruby, $d(10Dq)/dR=-366 \text{ cm}^{-1}/\text{pm}$.^{10,11} Results of $[10Dq(R_j)]_j$ are also collected in Table I, while the dependence of the p_j probabilities on the chromium content is portrayed in Fig. 2.

For a chromium concentration in the $0.1 < x < 0.25$ range the dominant centers are, as expected (Fig. 2), those corresponding to $j=0$ and $j=1$. It is worth noting that, comparing these two centers (Table I), the diminution in $10Dq$ for the $j=1$ center mainly comes from the decrease in Δ_R (equal to

TABLE I. $10Dq$ values (in cm^{-1}) calculated for the eight centers depicted in Fig. 1. $[10Dq(R_0)]_j$ are the values corresponding to keep the mean $\text{Cr}^{3+}\text{-O}^{2-}$ distance at $R=196.5$ pm, whereas $[10Dq(R_j)]_j$ are the values in which the corrections due to the small increase in distance on passing from ruby to pure Cr_2O_3 have been taken into account (see the main text).

j	0	1	2	3	4	5	6	7
$[10Dq(R_0)]_j$	17917	17511	17877	17292	17389	17190	17175	17183
$[10Dq(R_j)]_j$	17917	17374	17739	17017	17114	16777	16763	16633

406 cm^{-1}) induced by the replacement of a close Al^{3+} ion by a *nearly silent* Cr^{3+} ion. A similar situation also holds for all $j > 2$ centers, as shown in Table I.

The calculated $10Dq$ value for every chromium concentration by means of Eq. (1) and the $[10Dq(R_j)]_j$ and p_j quantities gathered in Table I and Fig. 2, respectively, is depicted in Fig. 3 and compared to experimental results. It can be noticed that the $10Dq$ values calculated in this work (where no fitting parameters are employed) follow the experimental ones rather well.

The model developed in this work is based on the idea of a complex perturbed by close Al^{3+} ions replaced by Cr^{3+} ions. Though this model is, in principle, reasonable for a relatively low chromium content ($x < 0.20$), it also reproduces the experimental findings for higher x values. This situation is however not surprising when looking at experimental $10Dq$ values measured for $3d$ ions in *normal* cubic perovskites where $V_R(r)$ is practically flat in the complex region and thus the Δ_R contribution to $10Dq$ is negligible.¹⁹ It turns out that the $10Dq$ values measured for AMnF_3 ($A: \text{K, Rb}$) pure compounds and also for Mn^{2+} doped cubic perovskites (such as KMgF_3 or RbCdF_3) *all* follow the same law $10Dq = KR^{-n}$ with $n=4.7$ and thus $\text{RbCdF}_3:\text{Mn}^{2+}$ ($R=213 \pm 1$ pm; $10Dq=7150 \text{ cm}^{-1}$) and RbMnF_3 ($R=212$ pm; $10Dq=7500 \text{ cm}^{-1}$) do exhibit close $10Dq$ values.²⁴

The present work thus supports that a *main cause* behind the color shift in the $\text{Al}_2\text{O}_3 \cdot x\text{Cr}_2\text{O}_3$ solid solutions comes from the reduction in the internal electric field, $\mathbf{E}_R(\mathbf{r})$, due to the progressive replacement of close Al^{3+} ions by Cr^{3+} whose actual charge is much smaller. Therefore, although for ruby $\Delta_R/(10Dq)_V=0.13$, the *secondary* contribution to $10Dq$, due to $\mathbf{E}_R(\mathbf{r})$ and not considered in the ligand field

theory, plays a key role for understanding the color shift from ruby to the series of $\text{Al}_2\text{O}_3 \cdot x\text{Cr}_2\text{O}_3$ mixed crystals. As shown in Fig. 3 these changes have *already* been observed for Cr^{3+} concentrations down to 5%.^{5,6} The results of this work thus support that the *same cause* is responsible for the color shift in the $\text{Al}_2\text{O}_3 \cdot x\text{Cr}_2\text{O}_3$ series and also the distinct color displayed by ruby, emerald, or the chromium spinel. In the case of Cr^{3+} -based gemstones the different shape of $\mathbf{E}_R(\mathbf{r})$ reflects that the Al_2O_3 , $\text{Be}_3\text{Si}_6\text{Al}_2\text{O}_{18}$, and MgAl_2O_4 host lattices are not isomorphous.^{17,18}

The variation in the optical absorption spectrum along the $\text{Al}_2\text{O}_3 \cdot y\text{Cr}_2\text{O}_3$ series has been conjectured by other authors to arise from a change in bonding due to the second coordination sphere.²⁵ The present study supports that when $x < 0.20$ the *main* effect due to the $\text{Al}^{3+} \rightarrow \text{Cr}^{3+}$ substitution in the second coordination sphere is the reduction in the *electrostatic* field $\mathbf{E}_R(\mathbf{r})$ seen by the CrO_6^{9-} complex rather than changes in the covalency of that unit. Along this line it is worth noting that upon passing from $\text{KMgF}_3:\text{Mn}^{2+}$ to $\text{LiBaF}_3:\text{Mn}^{2+}$ $10Dq$ increases¹⁹ by 16% while the charge on manganese varies only by about 4%.

Finally, it is worthwhile to remark that for $\text{MgAl}_2\text{O}_4 \cdot x\text{MgCr}_2\text{O}_4$ or $\text{YAl}_2\text{O}_4 \cdot x\text{YCr}_2\text{O}_4$ mixed crystals the evolution of the optical absorption spectrum and $10Dq$ with the chromium content is similar to that found for $\text{Al}_2\text{O}_3 \cdot y\text{Cr}_2\text{O}_3$.^{6,26,27} For instance, $10Dq=18\,500 \text{ cm}^{-1}$ for $\text{MgAl}_2\text{O}_4:\text{Cr}^{3+}$ while $10Dq=17\,180 \text{ cm}^{-1}$ for pure MgCr_2O_4 .^{9,27} Although no EXAFS measurements have been carried out for the whole $\text{MgAl}_{2-x}\text{Cr}_x\text{O}_4$ series, however re-

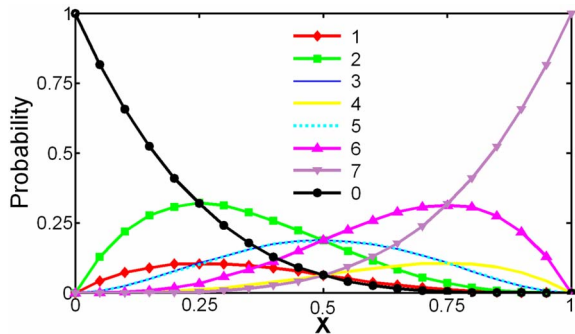


FIG. 2. (Color online) Probability of occurrence of the different cases represented in Fig. 1 as a function of Cr^{3+} ion concentration, x , in $\text{Al}_2\text{O}_3 \cdot x\text{Cr}_2\text{O}_3$ mixed crystals.

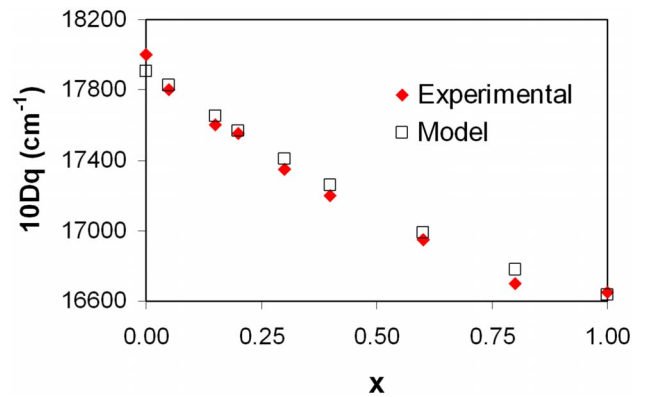


FIG. 3. (Color online) Experimental (red diamonds) and theoretical (white squares) values of $10Dq$ parameter as a function of Cr^{3+} ion concentration, x , in $\text{Al}_2\text{O}_3 \cdot x\text{Cr}_2\text{O}_3$. The experimental values have been taken from Ref. 5, and the theoretical ones have been derived using Eq. (1) of the main text.

cent EXAFS data on $\text{MgAl}_2\text{O}_4:\text{Cr}^{3+}$ give $R=198.0$ pm,^{26,27} which is again only 1.5 pm smaller than the corresponding value for pure MgCr_2O_4 . These results thus suggest that the cause behind the $10Dq$ change in the $\text{MgAl}_2\text{O}_4 \cdot x\text{MgCr}_2\text{O}_4$ series for relatively low chromium content is the same as that

found in the present study on $\text{Al}_2\text{O}_3 \cdot x\text{Cr}_2\text{O}_3$. Further work on this matter is now in progress.

The support by the Spanish Ministerio de Ciencia y Tecnología under Project No. FIS2006-02261 is acknowledged.

- ¹L. Bellaiche and D. Vanderbilt, Phys. Rev. Lett. **83**, 1347 (1999).
- ²M. Jansen and H. P. Letschert, Nature (London) **404**, 980 (2000).
- ³S. Lee and C. A. Randall, Appl. Phys. Lett. **92**, 111904 (2008).
- ⁴K. Nassau, *Color for Science, Art, and Technology* (Elsevier, Amsterdam, 1998).
- ⁵O. Schmitz-Du Mont and D. Reinen, Z. Elektrochem. **63**, 978 (1959).
- ⁶D. Reinen, Struct. Bonding (Berlin) **6**, 30 (1969).
- ⁷C. P. Poole, Jr., J. Phys. Chem. Solids **25**, 1169 (1964).
- ⁸L. Pauling, *The Nature of the Chemical Bond* (Cornell University Press, Ithaca, 1960).
- ⁹R. G. Burns, *Mineralogical Applications of Crystal Field Theory* (Cambridge University Press, Cambridge, 1993).
- ¹⁰S. J. Duclos, Y. K. Vohra, and A. L. Ruoff, Phys. Rev. B **41**, 5372 (1990).
- ¹¹J. M. García-Lastra, M. T. Barriuso, J. A. Aramburu, and M. Moreno, Phys. Rev. B **72**, 113104 (2005).
- ¹²M. G. Brik and N. M. Avram, J. Phys.: Condens. Matter **21**, 155502 (2009).
- ¹³É. Gaudry, P. Sainctavit, F. Juillot, F. Bondioli, P. Ohresser, and I. Letard, Phys. Chem. Miner. **32**, 710 (2006).
- ¹⁴S. Watanabe, T. Sasaki, R. Taniguchi, T. Ishii, and K. Ogasawara, Phys. Rev. B **79**, 075109 (2009).
- ¹⁵D. Bravo and R. Bottcher, J. Phys.: Condens. Matter **4**, 7295 (1992).
- ¹⁶R. W. Terhune, J. Lambe, C. Kikuchi, and J. Baker, Phys. Rev. **123**, 1265 (1961).
- ¹⁷J. M. García-Lastra, J. A. Aramburu, M. T. Barriuso, and M. Moreno, Phys. Rev. B **74**, 115118 (2006).
- ¹⁸J. M. García-Lastra, M. T. Barriuso, J. A. Aramburu, and M. Moreno, Phys. Rev. B **78**, 085117 (2008).
- ¹⁹A. Trueba, J. M. García-Lastra, M. T. Barriuso, J. A. Aramburu, and M. Moreno, Phys. Rev. B **78**, 075108 (2008).
- ²⁰C. Sousa, C. de Graaf, and F. Illas, Phys. Rev. B **62**, 10013 (2000).
- ²¹ q_n has been taken as the charge of the central M ion of the $M_{27}\text{O}_{42}^{3-}$ supercluster. Details of the calculation: PW91 exchange correlation functional. All electron calculations (no frozen core). TZP [triple- ζ Slater-type orbitals plus one polarization function] basis set.
- ²²G. te Velde, F. M. Bickelhaupt, E. J. Baerends, C. Fonseca Guerra, S. J. A. van Gisbergen, J. G. Snijders, and T. Ziegler, J. Comput. Chem. **22**, 931 (2001).
- ²³It has been assumed that $R_j = 1.965 + n_j \frac{1.98 - 1.965}{4}$, where n_j is the number of Al^{3+} ions replaced by Cr^{3+} ions.
- ²⁴F. Rodriguez and M. Moreno, J. Chem. Phys. **84**, 692 (1986).
- ²⁵D. Reinen, M. Atanasov, and S. L. Lee, Coord. Chem. Rev. **175**, 91 (1998).
- ²⁶A. Juhin, G. Calas, D. Cabaret, L. Galois, and J. L. Hazemann, Phys. Rev. B **76**, 054105 (2007).
- ²⁷A. Juhin, Ph.D. thesis, Université Paris VI-Pierre et Marie Curie, Paris, 2008.